

Dynamic transitions and resonances in Josephson-junction arrays under oscillating magnetic fields

Gun Sang Jeon

Center for Strongly Correlated Materials Research, Seoul National University, Seoul 151-747, Korea

Hyun Jin Kim and M.Y. Choi

Department of Physics and Center for Theoretical Physics, Seoul National University, Seoul 151-747, Korea

Beom Jun Kim and Petter Minnhagen

Department of Theoretical Physics, UmeåUniversity, 901 87 Umeå, Sweden

We investigate dynamic transitions and stochastic resonance phenomena in two-dimensional fully frustrated Josephson-junction arrays driven by staggered oscillating magnetic fields. As the temperature is lowered, the dynamic order parameter, defined to be the average staggered magnetization, is observed to acquire nonzero values. The resulting transition is found to belong to the same universality as the equilibrium Z_2 transition for small driving amplitudes while large driving fields appear to induce deviation from the universality class. The transition is also manifested by the stochastic resonance peak of the signal-to-noise ratio, which develops above the transition temperature.

PACS numbers: 74.50.+r, 74.25.Nf, 05.40.-a

The two-dimensional (2D) fully frustrated XY model, which provides a good description of the fully frustrated Josephson-junction array (FFJJA), has attracted much attention for the past decades, with regard to the Z_2 symmetry in addition to the $U(1)$ symmetry present in the system.¹⁻³ Extensive studies have been devoted to the nature of the equilibrium transition in the system, leading to general consensus on double transitions with some controversy as to the critical behavior of the Z_2 transition.^{2,3} Recently, the kinetic Ising model, which is a prototype model with the Z_2 symmetry, has been examined in the presence of oscillating magnetic fields.⁴⁻⁸ It has been revealed that spontaneous symmetry breaking takes place for finite strength of the oscillating field⁴⁻⁶ and that in two dimensions the transition belongs to the same universality class as the equilibrium 2D Ising transition.⁶ The signal-to-noise ratio (SNR) has also been found to exhibit double peaks,⁷ one above the transition temperature and the other below the transition temperature, the emergence of which has been explained in terms of the time-scale matching between the inherent relaxation time of the system and the external periodic driving.⁸ Such interesting results in the kinetic Ising model invokes interest in the dynamics of the FFJJA, which possesses the same Z_2 symmetry as the Ising model together with the additional continuous $U(1)$ symmetry. Furthermore, unlike the Ising model, the FFJJA has real intrinsic dynamics derived from the Josephson relations and thus grants direct experimental realizations;⁹ this makes the study of the FFJJA more attractive. It is a challenge to prepare oscillating fields which couples relevantly to the Z_2 degrees of freedom in the FFJJA. One possible realization may be provided by a periodic array of magnetic particles¹⁰ which is placed under the FFJJA and driven back and forth periodically.⁸ There have been some stud-

ies on the dynamic properties of the FFJJA,^{11,12} and very recently dynamic transitions were investigated in the FFJJA driven by uniform dc current.¹³ However, no results are available yet about dynamic transitions and stochastic resonance (SR) phenomena in the presence of oscillating fields.

This paper investigates the dynamic behavior of the FFJJA in the presence of the transverse magnetic field, which is staggered in space and periodic in time, with attention paid to the dynamic transition and SR phenomena. At low temperatures the chirality in the FFJJA displays antiferromagnetic ordering, to which the staggered oscillating field plays the same role as the oscillating field in the kinetic Ising model. To describe the dynamic transition to the antiferromagnetic ordering, we define the dynamic order parameter as the staggered magnetization averaged over one period of the (staggered) driving field, and examine its behavior with respect to the amplitude and the frequency of the driving field as well as the temperature. For small driving amplitudes, the scaling plot strongly indicates that the transition belongs to the same universality as the equilibrium Z_2 transition. On the other hand, as the driving amplitude is raised, apparent deviations can be observed in the scaling plot, suggesting a universality class different from the Z_2 one. We also examine the SNR and find a peak above the transition temperature, disclosing the SR present in the system. The absence of the lower peak is discussed in relation to the relaxation time of the system.

We begin with the equations of motion for the phases $\{\phi_i\}$ of the superconducting order parameters in superconducting grains forming an $L \times L$ square lattice. In the resistively-shunted-junction model with the fluctuating twist boundary conditions,¹⁴ they read:

$$\sum_j' \left[\frac{d\tilde{\phi}_{ij}}{dt} + \sin(\tilde{\phi}_{ij} - \mathbf{r}_{ij} \cdot \mathbf{\Delta}) + \eta_{ij} \right] = 0, \quad (1)$$

where the primed summation runs over the nearest neighbors of grain i . We have used the abbreviations $\tilde{\phi}_{ij} \equiv \phi_i - \phi_j - A_{ij}$ and $\mathbf{r}_{ij} \equiv \mathbf{r}_i - \mathbf{r}_j$ with $\mathbf{r}_i = (x_i, y_i)$ denoting the position of grain i , and expressed the energy and the time in units of $\hbar I_c/2e$ and $\hbar/2eRI_c$, respectively, with the critical current I_c and the shunt resistance R . The thermal noise current η_{ij} is assumed to be white satisfying $\langle \eta_{ij}(t+\tau)\eta_{kl}(t) \rangle = 2T\delta(\tau)(\delta_{ik}\delta_{jl} - \delta_{il}\delta_{jk})$ at temperature T and the dynamics of the twist variables $\mathbf{\Delta} \equiv (\Delta_x, \Delta_y)$ is governed by the equations

$$\frac{d\Delta_a}{dt} = \frac{1}{L^2} \sum_{\langle ij \rangle_a} \left[\sin(\tilde{\phi}_{ij} - \Delta_a) - \frac{dA_{ij}}{dt} \right] + \eta_{\Delta_a}, \quad (2)$$

where L is the system size, $\sum_{\langle ij \rangle_a}$ denotes the summation over all nearest-neighboring pairs in the a -direction ($a = x, y$), and η_{Δ_a} satisfies $\langle \eta_{\Delta_a}(t+\tau)\eta_{\Delta_a}(t) \rangle = (2T/L^2)\delta(\tau)$. The gauge field $A_{ij} (= -A_{ji})$, which incorporates the effects of the transverse magnetic field, takes the form

$$A_{ij} = \begin{cases} 0 & \text{for } \mathbf{r}_j = \mathbf{r}_i + \hat{\mathbf{x}}, \\ \pi x_i + \pi(-1)^{x_i+y_i} f_0 \sin \Omega t & \text{for } \mathbf{r}_j = \mathbf{r}_i + \hat{\mathbf{y}}, \end{cases} \quad (3)$$

which corresponds to the combined uniform constant and staggered oscillating fields. The frustration, i.e., the flux in units of the flux quantum through the plaquette at the dual lattice site $\mathbf{R}_i \equiv \mathbf{r}_i + (1/2)(\hat{\mathbf{x}} + \hat{\mathbf{y}})$ thus consists of the uniform full dc component and the staggered ac component of amplitude f_0 and frequency Ω :

$$f_{\mathbf{R}_i} = \frac{1}{2} + (-1)^{x_i+y_i} f_0 \sin \Omega t. \quad (4)$$

For the study of the transition associated with the Z_2 symmetry in the FFJJA, it is convenient to consider the chirality

$$C(\mathbf{R}, t) \equiv \text{sgn} \left[\sum_P \sin(\tilde{\phi}_{ij}(t) - \mathbf{r}_{ij} \cdot \mathbf{\Delta}(t)) \right] \quad (5)$$

and the staggered magnetization

$$m(t) \equiv \frac{1}{L^2} \sum_{\mathbf{R}} (-1)^{x_i+y_i} C(\mathbf{R}, t), \quad (6)$$

where \sum_P denotes the directional plaquette summation of links around dual lattice site \mathbf{R} . To probe the dynamic transition in the presence of an oscillating field, we define the dynamic order parameter as the staggered magnetization averaged over the period of the field⁴

$$Q = \frac{\Omega}{2\pi} \left| \oint m(t) dt \right|. \quad (7)$$

In numerical simulations, the sets of equations of motion (1) and (2) have been integrated via the modified Euler

method with time steps $\Delta t = 0.05$. We have followed an annealing schedule with the equilibration time at least 500 periods at each temperature.

In the fully frustrated array, it is well known that its Z_2 symmetry produces two kinds of antiferromagnetic chirality ordering at zero temperature. The staggered driving field in Eq. (4), which favors one of the two ground states in the first half of a period and the other in the latter half, is expected to induce oscillations between the two ground states when the driving amplitude is sufficiently large. Figure 1 displays the time evolution of the staggered magnetization $m(t)$ at zero temperature, with the initial condition $m(t=0) = 1$, for various amplitudes of the driving field. For $f_0 < f_c$ (which is equal to 0.5 regardless of the driving frequency), the system remains in the state with $m = 1$ even in the presence of the driving field. As the amplitude is increased beyond the critical value f_c , the system is driven out of the $m = 1$ state, giving rise to oscillations in the staggered magnetization between $m = \pm 1$. It is interesting that the residence time in one state is different from that in the other. Accordingly, for $f_0 > f_c$, although the dynamic order parameter is not unity, it still does not vanish. From Eq. (4), we expect the array to stay at the $m = -1$ state only during the interval given by $f_0 \sin \Omega t < -1/2$; this leads to the dynamic order parameter for $f_0 > f_c$,

$$Q(f_0) = 1 - \frac{2}{\pi} \cos^{-1} \frac{1}{2f_0}, \quad (8)$$

which depends on the driving amplitude f_0 but not on the driving frequency Ω . In Fig. 2 we plot the dynamic order parameter Q versus the amplitude f_0 at zero temperature. The numerical data indeed agree very well with the analytical results given by Eq. (8), establishing the validity of the analytical argument.

At sufficiently high temperatures, the influence of the oscillating field may be neglected and the staggered magnetization fluctuates randomly with time, resulting in the null value of the dynamic order parameter. Accordingly, we expect that there is a transition between the ordered state at low temperatures and the disordered state at high temperatures. Figure 3, in which the behavior of $\langle Q \rangle$, the ensemble average of the dynamic order parameter, with the temperature is plotted for various driving frequencies, demonstrates clearly the existence of such a transition: The dynamic order parameter, starting from zero at high temperatures, develops as the temperature is reduced. It then grows rapidly around a certain temperature, from which the transition temperature T_c can be inferred, and saturates eventually as the temperature approaches zero. The saturation value assumed by the dynamic order parameter at zero temperature is unity for $f_0 < f_c$, as shown in Fig. 3(a); for $f_0 > f_c$, it is given by Eq. (8) [see Fig. 3(b)]. It is indicated that in both cases the transition temperature becomes higher with the increase of the driving frequency Ω .

The transition temperature in the thermodynamic limit can be conveniently obtained from the consideration of Binder's cumulant¹⁵

$$U_L = 1 - \frac{\langle Q^4 \rangle}{3\langle Q^2 \rangle^2}. \quad (9)$$

This quantity is known to be independent of the system size at the transition temperature T_c , which allows one to estimate the transition temperature by the crossing point of the cumulants for different sizes. [See the inset of Fig. 4, in which the cumulant is plotted as a function of the temperature T for various system sizes.] In this manner we have estimated the transition temperature for various values of the driving amplitude f_0 and frequency Ω , and show in Fig. 4 the resulting phase diagram for the dynamic transition on the T - f_0 plane. For given frequency Ω , the transition temperature decreases monotonically with the driving amplitude f_0 , similarly to the case of the kinetic Ising model. As Ω is increased, on the other hand, the transition temperature also increases, expanding the ordered region on the T - f_0 plane. It is thus concluded that high-frequency driving helps to establish order whereas large-amplitude one tends to suppress order. It should be noted here that the cooling and heating curves for the dynamic order parameter do not exhibit any hysteresis in the strong-field regime. This apparently indicates the absence of a tricritical point, above which the system undergoes a discontinuous transition, and contrasts sharply with the kinetic Ising models under oscillating fields both in the mean-field version⁴ and in two dimensions.⁵

Regarding the nature of the transition, it is revealing to recall that the system at zero temperature, residing in one of the two ($m = \pm 1$) states for $f_0 < f_c$, displays oscillations between the two states as f_0 is raised beyond f_c . This suggests that the critical behavior near the transition may change qualitatively at $f_0 = f_c$. To probe such possibility, we consider the scaling law for the dynamic order parameter¹⁶

$$\langle Q \rangle = L^{-\beta/\nu} F((T - T_c)L^{1/\nu}) \quad (10)$$

with appropriate scaling function $F(x)$ and plot $\langle Q \rangle L^{\beta/\nu}$ versus $(T - T_c)L^{1/\nu}$ in Fig. 5 for various sizes. Figure 5(a) shows the best collapse of the numerical data for $f_0 = 0.3$, yielding the critical exponents $\beta = 0.10 \pm 0.02$ and $\nu = 0.82 \pm 0.05$; these values provide good collapse in the whole range of $f_0 < f_c$. Note the good agreement of the obtained exponents with those of the equilibrium transition³, which strongly suggests that the dynamic transition at weak driving fields belongs to the same universality class as the equilibrium Z_2 transition in the fully frustrated XY model. Similar conclusion was also reached in the kinetic Ising model under oscillating fields.⁶ For $f > f_c$, on the other hand, the scaling plot with the same critical exponents, apparently does not collapse into a single curve. Such dispersion, which begins to show up around $f_0 = f_c$, indicates deviation

of the critical behavior from that of the equilibrium Z_2 transition, manifesting the expected change of the nature of the transition at $f_0 = f_c$. Instead the data fit well to the scaling form in Eq. (10) with $\beta = 0.36 \pm 0.08$ and $\nu = 0.9 \pm 0.1$, as shown in Fig. 5(b) for $f_0 = 0.8$. These values of the exponents, estimated from the best collapse for $f_0 > f_c$, turn out to be independent of f_0 within numerical errors.

Finally, to explore the possibility of the SR phenomena in the system, we compute the SNR defined to be

$$\text{SNR} = 10 \log_{10} \left[\frac{S}{N} \right]. \quad (11)$$

Here the signal S is given by the peak value of the power spectrum of $m(t)$ at the driving frequency Ω while the background noise level N is estimated by the average power spectrum around the signal peak. Figure 6 displays the SNR versus the temperature (a) for weak driving ($f_0 = 0.1$) and (b) for strong driving ($f_0 = 0.6$). For $f_0 < f_c$ shown in (a), the SNR peak emerges above the transition temperature and signals the presence of the SR in the system, which is reminiscent of the SR behavior of the kinetic Ising field in weak oscillating fields.⁷ For $f_0 > f_c$ one may expect monotonic decrease of the SNR with the temperature since the array has inherent oscillations of the staggered magnetization $m(t)$ even at zero temperature. This expectation appears to be valid at low temperatures as shown in Fig. 6(b). As the temperature is raised, however, the SNR changes its behavior: Sharp decrease of the SNR turns into gradual increase seemingly at the transition temperature and into gradual decrease again above the transition temperature, giving rise to a small broad peak.

Here it is of interest that the system exhibits no peak below the dynamic transition, which seems to be in contradiction to the prediction of the double SR peaks, one below and the other above the dynamic transition temperature.⁸ The origin of the double peaks is the time-scale matching between the external periodic driving and the relaxation time associated with the transition in the system. To disclose the origin of the discrepancy, we examine the relaxation of the system from random initial configurations at given temperatures, and estimate the relaxation time τ by fitting $Q(t) - \langle Q \rangle$ to the exponential form $\sim \exp[-t/\tau]$ in the long-time scale. The inverse of the resulting relaxation time for $f_0 = 0.1$ is shown in Fig. 7. As expected, the inverse relaxation time increases with the temperature above T_c , which is consistent with the critical behavior

$$\tau^{-1} \sim (T - T_c)^{\nu z} \quad (12)$$

with the critical exponents given by the equilibrium values $\nu = 0.813 \pm 0.005$ and $z = 2.17 \pm 0.04$.¹² Thus supported again is the proposition that the dynamic transition under weak driving fields belongs to the same universality class as the equilibrium transition. At low temperatures below T_c , on the other hand, it is observed

that the relaxation time is enhanced enormously. Due to such enhancement of the relaxation time below T_c , the system fails to match the external time scale, which is estimated to be $\tau^{-1} \approx 0.032$ from the SNR peak above T_c . The origin of the enhancement at low temperatures is not clear yet, but it can be attributed to the existence of a large number of metastable states associated with, e.g., domain-wall excitations, which cannot be observed in the mean-field system considered in Ref. 8. Indeed faceted domain walls have been pointed out to cause slow growth in the FFJJA below $T_R \approx 0.3$,¹⁷ where the enhancement of the relaxation-time data is conspicuous in Fig. 7. This strongly supports our argument concerning the failure of time-scale matching.

In summary, we have studied dynamic properties of the 2D FFJJA driven by staggered oscillating magnetic fields, paying attention to the dynamic transition and SR phenomena. To describe the dynamic transition to the antiferromagnetic ordering of the chirality in the system, we have introduced the dynamic order parameter, which is the staggered magnetization averaged over one period of the staggered driving field, and examined its behavior with respect to the amplitude and the frequency of the driving field as well as the temperature. The transition temperature has been computed by means of Binder's cumulants for various driving amplitudes and frequencies, and as a result, the phase diagram displaying boundaries of the dynamic transition has been obtained on the plane of the temperature and the driving amplitude for various driving frequencies. While the scaling analysis for weak driving has demonstrated the universality of the equilibrium Z_2 transition, a universality class different from the Z_2 one has been suggested for strong driving. We have also examined the SNR and found a peak above the transition temperature, disclosing the SR present in the system. The absence of the lower peak has been discussed in relation to the relaxation time of the system and attributed to the striking increase at low temperatures.

This work was supported in part by the Ministry of Education of Korea through the BK21 Program (H.J.K and M.Y.C.) and by the Swedish Natural Research Council through Contract No. F 5102-659/2001 (B.J.K. and P.M.).

- B **48**, 7438 (1993); Y.M.M. Knops, B. Nienhuis, H.J.F. Knops, and H.W.J. Blöte, *ibid.* **50**, 1061 (1994).
² J.-R. Lee, Phys. Rev. B **49**, 3317 (1994); P. Olsson, Phys. Rev. Lett. **75**, 2758 (1995); G.S. Jeon, S.Y. Park, and M.Y. Choi, Phys. Rev. B **55**, 14088 (1997).
³ S. Lee and K.-C. Lee, Phys. Rev. B **49**, 15184 (1994).
⁴ T. Tomé and M. J. de Oliveira, Phys. Rev. A **41**, 4251 (1990).
⁵ M. Acharyya, Phys. Rev. E **59**, 218 (1999).
⁶ G. Korniss, C.J. White, P.A. Rikvold, and M.A. Novotny, Phys. Rev. E **63**, 016120 (2000).
⁷ K.-T. Leung and Z. Néda, Phys. Rev. E **59**, 2730 (1999).
⁸ B.J. Kim, P. Minnhagen, H.J. Kim, M.Y. Choi, and G.S. Jeon, Europhys. Lett. **56**, 333 (2001).
⁹ For a review, see, e.g., *Macroscopic Quantum Phenomena and Coherence in Superconducting Networks*, edited by C. Giovannella and M. Tinkham (World Scientific, Singapore, 1995); Physica B **222**, 253 (1996).
¹⁰ J.I. Martín, M. Vélez, A. Hoffmann, I.K. Schuller, and J.L. Vicent, Phys. Rev. B **62**, 9110 (2000).
¹¹ K.K. Mon and S. Teitel, Phys. Rev. Lett. **62**, 673 (1989); J.S. Chung, K.H. Lee, and D. Stroud, Phys. Rev. B **40**, 6570 (1989); S. Kim and M.Y. Choi, *ibid.* **48**, 322 (1993).
¹² H.J. Luo, L. Schülke, and B. Zheng, Phys. Rev. Lett. **81**, 180 (1998).
¹³ V.I. Marconi and D. Domínguez, Phys. Rev. Lett. **87**, 017004 (2001).
¹⁴ B.J. Kim, P. Minnhagen, and P. Olsson, Phys. Rev. B **59**, 11506 (1999).
¹⁵ K. Binder, Phys. Rev. Lett. **47**, 693 (1981).
¹⁶ V. Privman and M.E. Fisher, Phys. Rev. B **30**, 322 (1984).
¹⁷ S.J. Lee, J.-R. Lee, and B. Kim, Phys. Rev. E **51**, R4 (1995). See also J.-R. Lee, S.J. Lee, B. Kim, and I. Chang, Phys. Rev. Lett. **79**, 2172 (1997).

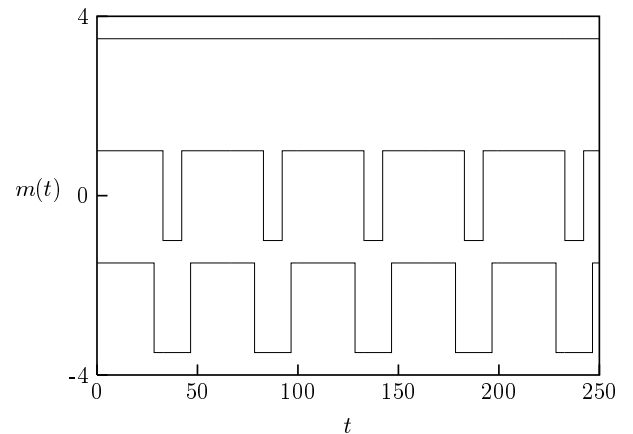


FIG. 1. Time evolution of the staggered magnetization at zero temperature for driving frequency $\Omega/2\pi = 0.02$ and amplitudes $f_0 = 0.4, 0.6$, and 1.2 from above. For clarity, the data corresponding to $f_0 = 0.4$ and 1.2 have been shifted by 1.5 upward and downward, respectively.

¹ S. Teitel and C. Jayaprakash, Phys. Rev. B **27**, 598 (1983); M.Y. Choi and S. Doniach, *ibid.* **31**, 4516 (1985); M. Yosefin and E. Domany, *ibid.* **32**, 1778 (1985); M.Y. Choi and D. Stroud, *ibid.* **32**, 5773 (1985); E. Granato, J.M. Kosterlitz, and J. Poulter *ibid.* **33**, 4767 (1986); J. Lee, J.M. Kosterlitz, and E. Granato, *ibid.* **43**, 11531 (1991); G. Ramirez-Santiago and J.V. José, Phys. Rev. Lett. **68**, 1224 (1992); E. Granato and M.P. Nightingale, Phys. Rev.

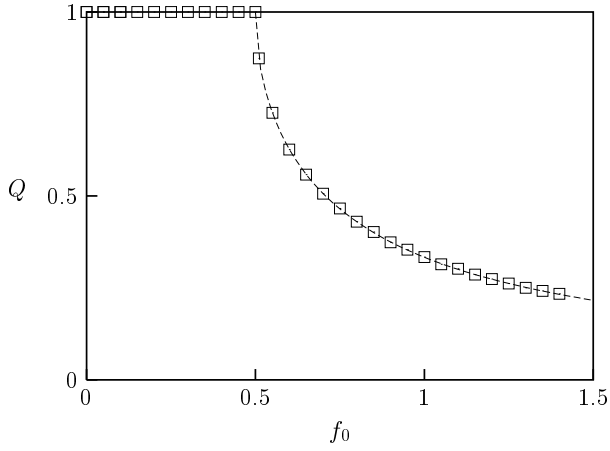


FIG. 2. Dynamic order parameter as a function of f_0 at zero temperature in the system of size $L = 16$ and with frequency $\Omega/2\pi = 0.02$. The dashed line represents the analytic result in Eq. (8).

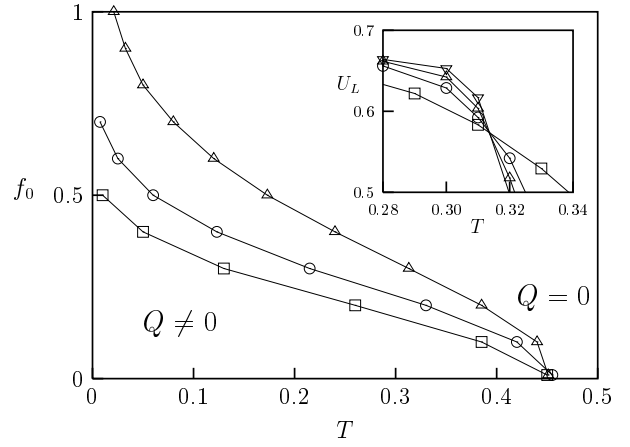
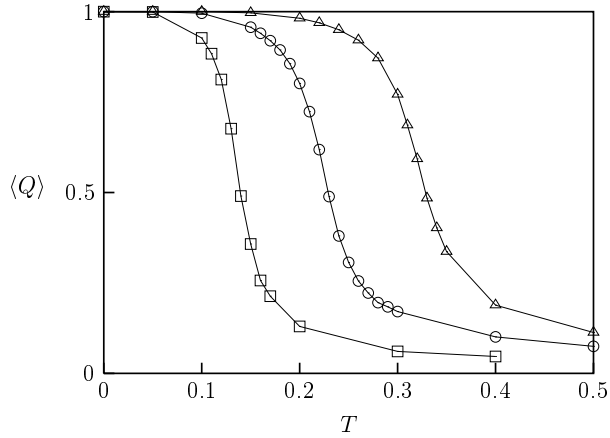
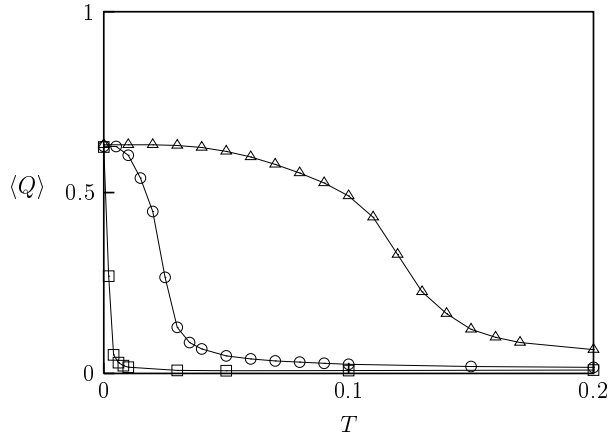


FIG. 4. Dynamic phase diagram on the $T-f_0$ plane for various driving frequencies $\Omega/2\pi = 0.02(\square)$, $0.04(\circ)$, $0.08(\triangle)$. The boundaries are determined by the crossing points of Binder's cumulant for several sizes $L = 8, 16, 24$, and 32 . Inset: Binder's cumulant U_L as a function of the temperature for $f_0 = 0.3$ and $\Omega/2\pi = 0.08$ in the system of size $L = 8(\circ)$, $16(\square)$, $24(\triangle)$, and $32(\nabla)$.

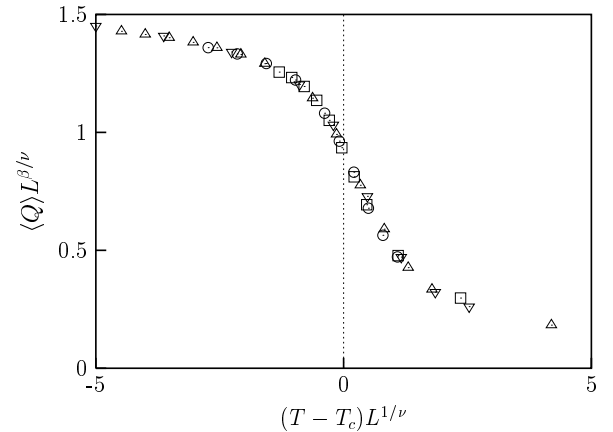


(a)

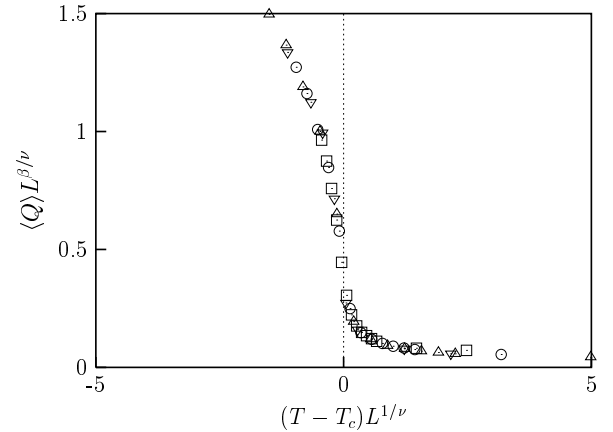


(b)

FIG. 3. Dynamic order parameter as a function of temperature T in the system of size $L = 16$ for various driving frequencies $\Omega/2\pi = 0.02(\square)$, $0.04(\circ)$, $0.08(\triangle)$ and (a) $f_0 = 0.3$; (b) $f_0 = 0.6$.

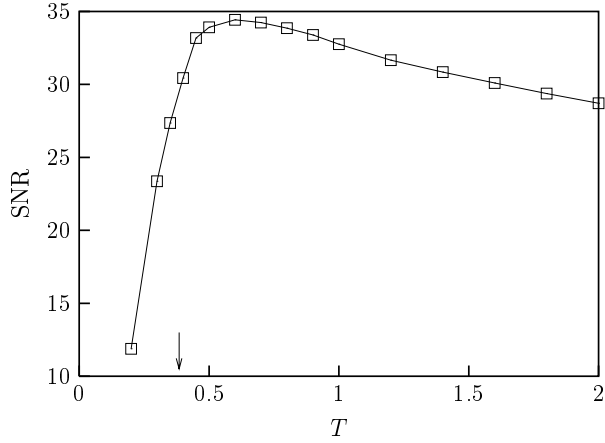


(a)

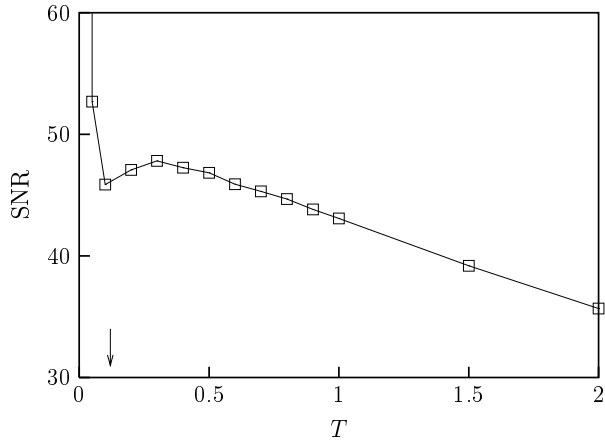


(b)

FIG. 5. Scaling plot of the dynamic order parameter versus the temperature for size $L = 8(\square)$, $16(\circ)$, $24(\triangle)$, and $32(\nabla)$ with $\Omega/2\pi = 0.08$ and (a) $f_0 = 0.3$; (b) $f_0 = 0.8$. The best collapse is obtained with (a) $\beta = 0.10$ and $\nu = 0.82$; (b) $\beta = 0.36$ and $\nu = 0.90$.



(a)



(b)

FIG. 6. Signal-to-noise ratio versus the temperature in the system of size $L = 16$ for (a) $f_0 = 0.1$ and $\Omega/2\pi = 0.02$; (b) $f_0 = 0.6$ and $\Omega/2\pi = 0.08$. The arrows indicate the positions of the transition temperatures.

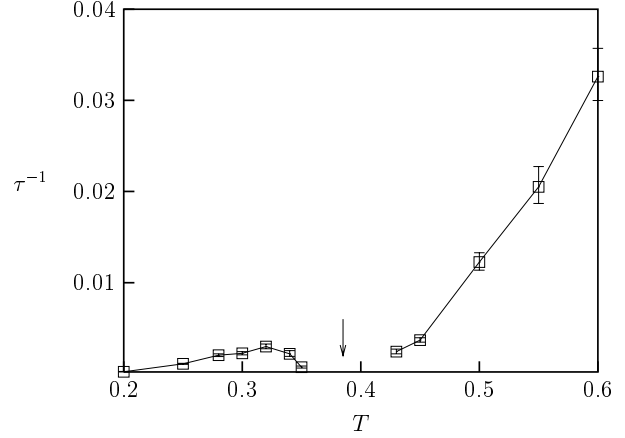


FIG. 7. Inverse of the relaxation time as a function of the temperature for $L = 16$, $f_0 = 0.1$, and $\Omega/2\pi = 0.02$. The arrow indicates the position of the transition temperature.